Journal of Inclusion Phenomena **1**, 105–123. 0167–7861/83/0012–0105$02.85.

Zeolite Inclusion Complexes

R. M. BARRER
Physical Chemistry Laboratories Imperial College, London S.W.7, England

(Received: 26 November 1982)

Abstract. Zeolites provide the largest and most useful family of porous host crystals, stable in the presence or absence of guest molecules. An account is given of their structural characteristics in terms of intracrystalline channels and cavities of molecular dimensions; their total intracrystalline pore volumes; and the intracrystalline distribution patterns of guest molecules, often present as clusters or filaments. The way in which the shape and size of the molecules relate to the shape and size of the apertures or windows giving access to the cavities, together with other factors such as cation location, then determine molecule sieving behaviour, which is discussed with reference to several types of zeolite sieve. The relation between diffusivity and molecular dimensions is also illustrated. A comparison between zeolites and clathrate host lattices shows that there are strong similarities of several kinds. Zeolites may form inclusion complexes with metals, salts and polar or non-polar molecules, examples of which are briefly considered, together with isotherms for some of these types of complex. An account of equilibrium and its formulation demonstrates the thermodynamic background and illustrates the degree of success which has been obtained in describing isotherms in terms of various models.

Key words: Zeolite inclusion complexes review.

1. Introduction: Porous Tectosilicates

The most stable and technically the most useful family of host crystals are the porous tectosilicates, which comprise the zeolites and several crystalline silicas having the same framework topologies as certain zeolites. About 60 different zeolite framework topologies are currently available and very many more have been constructed as models and await synthesis. This variety of structures owes its existence to the ease of linking tetrahedra of SiO_4 and AlO_4 to make numerous space patterns. In tectosilicates, every tetrahedron is linked by sharing each of its oxygens with one of four other tetrahedra. The number of space patterns which can be created is a problem in geometry and topology which is not yet comprehensively formulated, although a number of limited approaches have been very successful in exploring novel structures [1]. The number of patterns possible will be restricted only by imposing upper limits to the unit cell size. Among the largest unit cells so far are those of paulingite (cubic; a = 35.1 Å) and the synthetic zeolite $Na,N(CH_3)_4-V$ (cubic; a = 37.0 Å). Unit cells many times greater in volume than these, because of their complexity, seem increasingly unlikely to be synthesised. Thus, irrespective of the topological possibilities, there may be a practical limit to the numbers of zeolites eventually prepared.

2. Zeolite Cavities and Channels

Zeolites were first synthesised at temperatures above 100 °C, often at several hundred degrees. However, for many species one need not go above 100 °C so that hydrothermal formation merges into formation at atmospheric pressures, under conditions familiar to chemists. Another trend has been towards zeolites with very high SiO_2/Al_2O_3 ratios and,

Table I. Porous crystalline silicas

Silica	Isostructural zeolite	Isostructural clathrate
Melanophlogite [2]	—	Gas hydrate Type I
—	Zeolite ZSM-39 [6]	Gas hydrate Type II
Silicalite I [3]	Zeolite ZSM-5 [7,8]	—
Silicalite II [4]	Zeolite ZSM-11 [7,8]	—
Faujasite silica [5]	Faujasite	—

in the limit, to Al-free crystalline silicas having the same topologies as certain zeolites. Crystalline silicas, porous on the scale of molecular dimensions, are exemplified in Table I. Like a gas hydrate of Type I, melanophlogite can be constructed by stacking pentagonal dodecahedra and tetradecahedra with 12 × 5-ring and 2 × 6-ring faces. The stacked polyhedra share 5-ring faces. (Table II) Zeolite ZSM-39 is constructed similarly from stacked dodecahedra with pentagonal faces and hexadecahedra with 12 × 5-ring and 4 × 6-ring faces.

Table II. Examples of polyhedral cavities found in zeolites and porous silicas [13]

Polyhedron	Faces	Approx. free dimensions (in Å)	Present in
6-hedron (cube)	6 × 4-rings	—	Zeolite A
8-hedron (hexagonal prism)	2 × 6-rings 6 × 4-rings	2.3 in plane of 6-ring	Faujasite, ZK-5, chabazite, erionite, offretite, levynite
10-hedron (octagonal prism)	2 × 8-rings 8 × 4-rings	4.5 in plane of 8-ring	Paulingite, RHO
11-hedron	5 × 6-rings 6 × 4-rings	4.7 along *c*-axis 3.5 normal to *c*	Cancrinite, zeolite L, erionite, offretite, losod
12-hedron	12 × 5-rings	—	ZSM-39, melanophlogite
14-hedron type I	8 × 6-rings 6 × 4-rings	6.6 for inscribed sphere	Sodalite, faujasite, zeolite A, liottite, afghanite
14-hedron type II	3 × 8-rings 2 × 6-rings 9 × 4-rings	6.0 along *c* 7.4 normal to *c* (gmelinite)	Gmelinite, offretite mazzite
14-hedron type III	2 × 6-rings 12 × 5-rings	—	Melanophlogite
16-hedron	4 × 6-rings 12 × 5-rings	—	ZSM-39
17-hedron type I	3 × 8-rings 5 × 6-rings 9 × 4-rings	9.0 along *c*, 7 to 7.3 normal to *c*	Levynite
17-hedron type II	11 × 6-rings 6 × 4-rings	7.7 along *c* 6.4 normal to *c* (losod)	Liottite, losod
18-hedron	6 × 8-rings 12 × 4-rings	10.8 by 6.6 (6.6 between centre planes of opposite 8-rings) (ZK-5)	ZK-5, paulingite
20-hedron	6 × 8-rings 2 × 6-rings 12 × 4-rings	11 along *c* 6.5 normal to *c*	Chabazite

Table 2 (continued)

Polyhedron	Faces	Approx. free dimensions (in Å)	Present in
23-hedron type I	6 × 8-rings 5 × 6-rings 12 × 4-rings	15 along *c* 6.3 normal to *c*	Erionite
23-hedron type II	17 × 6-rings 6 × 4-rings	—	Afghanite, liottite
26-hedron type I	6 × 8-rings 8 × 6-rings 12 × 4-rings	11.4 for inscribed sphere (zeolite A)	Paulingite, zeolite A, ZK-5, RHO
26-hedron type II	4 × 12-rings 4 × 6-rings 18 × 4-rings	11.8 for inscribed sphere	Faujasite

Silicalites I and II are the silica end members of ZSM-5 and 11, respectively, and faujasite silica is the silica end member of faujasite. Unlike the other porous silicas, it is prepared indirectly by high temperature reaction of Na–Y (a synthetic faujasite) with $SiCl_4$ vapour. In the reaction Si replaces all framework Al and yields $AlCl_3$, NaCl and $NaAlCl_4$ [5] e.g.

$$Na_{52}[Al_{52}Si_{140}O_{384}] + 52SiCl_4 \rightarrow Si_{192}O_{384} + 52AlCl_3 + 52NaCl.$$

The structures of the frameworks of silicalite I, silicalite II and faujasite silica, and of the corresponding zeolites, are shown in Figures 1 [9], 2 [10] and 3 [11], respectively. As sorbents, these silicas tend to be hydrophobic, in contrast with the zeolites which are hydrophilic, because of the anionic charge of the aluminosilicate frameworks and its electrochemical equivalent of intracrystalline cations.

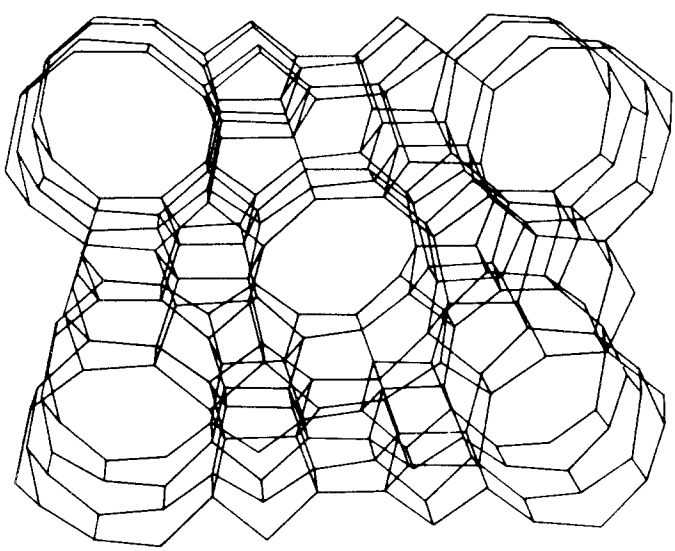

Fig. 1. The aluminosilicate framework structure of zeolite ZSM-5 [9]. In Figure 1 to 5 Al or Si atoms are centred at each corner and O atoms are centred near but not at the mid-point of each edge.

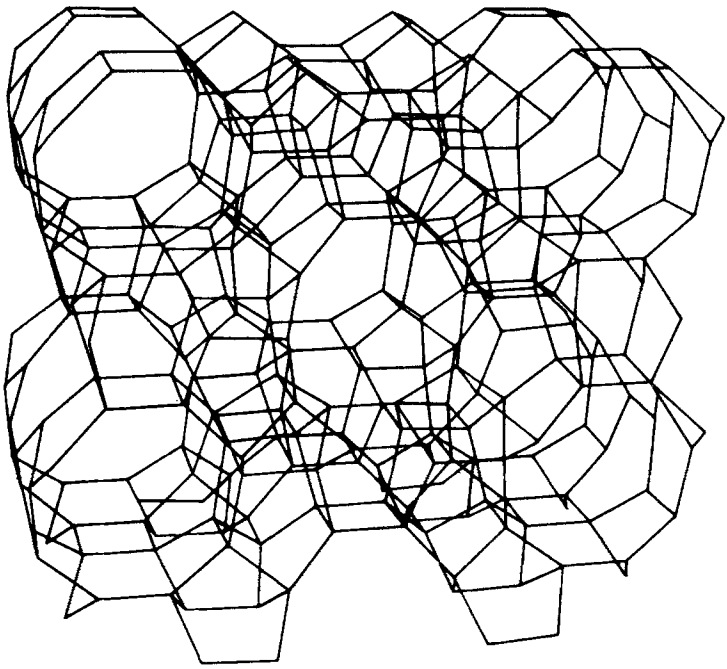

Fig. 2. The aluminosilicate framework of zeolite ZSM-11 [10].

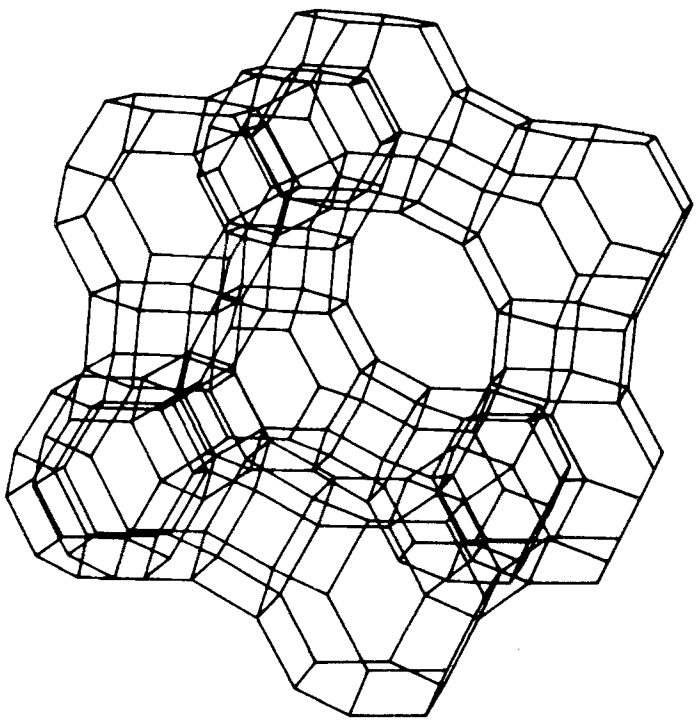

Fig. 3. The aluminosilicate framework of faujasite [11].

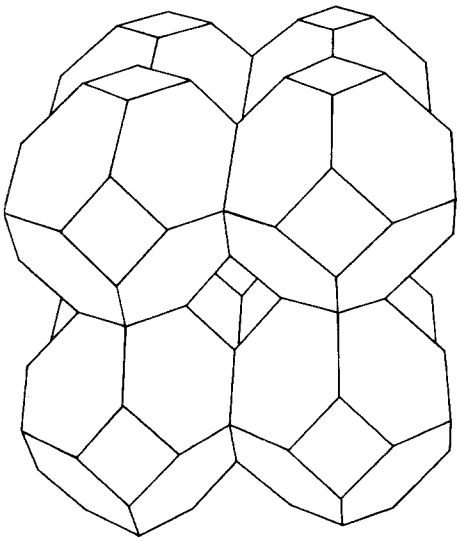

Fig. 4. The stacking of 14-hedra of type I in 8-fold co-ordination as found in the sodalite framework [12].

Many zeolites have frameworks which can be constructed by stacking polyhedral cavities with certain faces shared with like or unlike cavities. Figure 4 [12] shows the stacking in sodalite where 14-hedral cavities are stacked in 8-fold co-ordination with shared 6-ring faces. Examples of the cages found in zeolites are given in Table II, [13] with some of the zeolites in which they occur. Figure 5 [14] illustrates the contours of several such polyhedra.

If one measures the intracrystalline pore volumes as the volumes of liquid water which can be distilled from the crystals by heat and evacuation, one obtains the representative values given in Table III. In the most porous zeolites, about 50% of the volume of each crystal is pore space available to water and often to many other guest molecules. This pore space is parcelled up into cavities and/or channels of molecular dimensions. The resultant pathways through which guest molecules of the right shape and size can diffuse can be considered in three categories:

(1) All pathways are parallel noninterconnected channels (1-dimensional channel systems as in mordenite, mazzite, laumontite or zeolite L).
(2) The pathways, whether parallel or not, are interconnected to give 2-dimensional channel systems, i.e., the guest molecules may migrate in planes but not from one plane to another (heulandite, levynite, stilbite and ferrierite).
(3) The pathways may be so interconnected as to allow migration of guest molecules in 3-dimensions (chabazite, erionite, zeolite A, faujasite and zeolites ZSM-5, RHO and ZK-5).

The channel geometries, in whichever of the above three categories they fall, are different for every framework topology. The guest molecules saturating the crystals are distributed according to the spatial geometry of the channels. In 1-dimensional pathway systems they are present as parallel filaments supported by the channel walls. For example, in zeolite L there are narrow points or windows along each channel having openings of about 7.1 Å free diameter alternating with bulges of about 12 Å free diameter. Thus, the guest molecules form

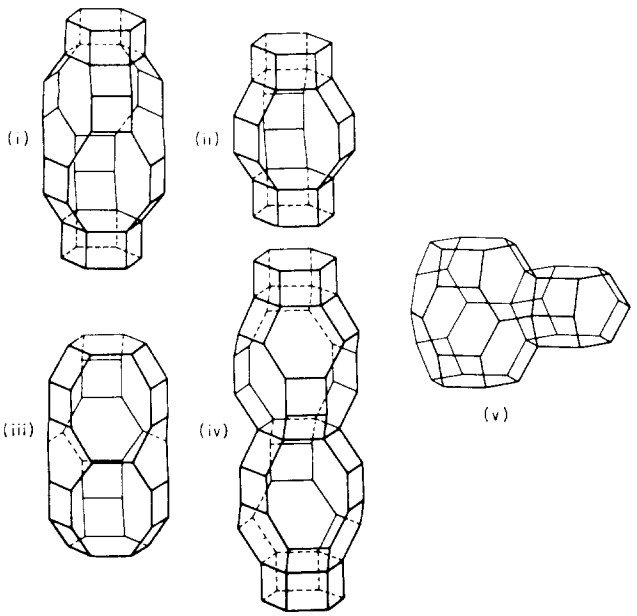

Fig. 5. Some polyhedral voids found in zeolites [14]. (i) The chabazite 20-hedron, capped by hexagonal prisms; (ii) the gmelinite 14-hedron of type II; (iii) the erionite 23-hedron; (iv) the levynite 17-hedron of type I; (v) the losod 17-hedron of type II with associated 11-hedral cancrinite cage.

Table III. Intracrystalline pore volumes V_i of some zeolites ($cm^3\ cm^{-3}$ of crystal) estimated as volume of liquid water displaceable

Zeolite	V_i	Zeolite	V_i	Zeolite	V_i
Analcime	0.18	Phillipsite	0.30	Sodalite hydrate	0.34
Wairakite	0.18	Harmotome	0.36	Cancrinite hydrate	0.34
Mordenite	0.26	Gismondine	0.47	Losod	0.37
Ferrierite	0.24	Garronite	0.41	Laumontite	0.35
Dachiardite	0.26	Yugawaralite	0.30	Faujasite	0.53
Epistilbite	0.34	Chabazite	0.48	Zeolites ZSM-3 and 2	~0.53
Bikitaite	0.20	Gmelinite	0.43	Paulingite	0.48
Natrolite	0.21	Erionite	0.36	Zeolite A	0.47
Thomsonite	0.32	Offretite	0.34	Zeolite RHO	0.48
Heulandite	0.35	Levynite	0.42	Zeolite ZK-5	0.45
Brewsterite	0.32	Mazzite	0.37	Zeolite N	~0.35
Stilbite	0.38	Zeolite L	0.28		

liquid-like beads in the bulges connected into filaments through the 7.1 Å apertures with other beads. In faujasite, 26-hedra of type II of a free diameter of about 12 Å are connected through 12-ring windows of free diameter ~ 7.4 Å to one each of four other 26-hedra, giving a channel pattern like that of the bonds in diamond. Liquid-like beads of guest molecules in each 26-hedron are connected through each window to four other beads, and so on. The smaller the free diameter of the connecting windows and the larger the guest molecule, the more isolated each molecular cluster becomes from its neighbours, while the smaller the cavity

and/or the larger the guest molecule the fewer are the molecules per cluster. Thus, in the 14-hedra of sodalite hydrate, the windows linking a given 14-hedron to one of eight like 14-hedra are 6-rings of free diameter ~ 2.1 Å. Each 14-hedron has a free diameter of about 6.6 Å. It can accommodate a cluster of four H_2O molecules (van der Waals diameter ~ 2.8 Å), which is more or less isolated from other such clusters by the narrowness of the windows. The water clusters can be removed by heat and evacuation and at high temperature and pressure of Ar or Kr (of diameters ~ 3.83 and ~ 3.94 Å respectively) can

Table IV. Cluster sizes at saturation of cavities in several zeolites [16]

Zeolite	Cavities	Guest molecules per cavity
Chabazite	20-hedra (6 × 8-rings 2 × 6-rings 12 × 4-rings)	12 – 14 H_2O ~7.7 NH_3 ~6 Ar,N_2,O_2 ~4.9 CH_3NH_2 ~4.3 CH_3Cl ~3.1 CH_2Cl_2 ~2.0 I_2
Zeolite A	26-hedra, type I (6 × 8-rings 8 × 6-rings 12 × 4-rings)	~29 H_2O (25 + 4) [a] 19 – 20 NH_3 14 – 16 Ar,N_2,O_2 ~15 H_2S ~12 CH_3OH ~10 SO_2 ~9 CO_2 ~5.5 I_2 ~5.4 *n*-C_3H_7OH ~4 *n*-C_4H_{10}
Faujasite	26-hedra, type II (4 × 12-rings 4 × 6-rings 18 × 4-rings)	~32 H_2O (28 + 4) [a] 17 – 19 Ar,N_2,O_2 ~7.5 I_2 ~7.8 CF_4 ~6.5 SF_6 ~5.8 C_2F_6 ~5.6 cyclopentane ~5.4 benzene ~4.6 toluene ~4.5 *n*-C_5H_{12} ~4.1 cyclohexane ~4.1 perfluorocyclobutane ~4.1 $C_2F_4Cl_2$ ~3.5 *n*-C_7H_{16} ~3.4 C_3F_8 ~2.9 *n*-C_4F_{10} ~2.8 *iso*-C_8H_{18} ~2.3 perfluoro-methylcyclo-hexane ~2.1 perfluoro-dimethyl-cyclohexane

[a] Four of the water molecules are thought to be in the 14-hedral sodalite cages also present in both zeolite A and faujasite.

be replaced by just one of either of these atoms [15]. There is not enough room in the 14-hedra for more than one such atom. One atom per cavity corresponds with interstitial solution as a limit to the larger clusters so often present in zeolitic solution. The numbers given in Table IV exemplify the sizes of molecular clusters at saturation found in three of the more porous zeolites. Contacts between clusters in chabazite or zeolite A can occur only through six 8-ring windows leading respectively from each 20-hedral or 26-hedral cavity to one each of six other like cavities. These windows have free diameters of about 3.6 × 3.7 Å for chabazite and 4.1 Å for zeolite A, taking the diameter of a lattice oxygen to be 2.70 Å. The corresponding situation with faujasite is as described earlier.

3. Molecule Sieving

The ease of migration of guest molecules within outgassed zeolites depends upon a number of factors:

(1) The size and shape of the guest molecule.
(2) The size and shape of the windows controlling entry to the channel system.
(3) The number, location and size of the exchangeable cations.
(4) The presence or absence of defects such as stacking faults which may narrow diffusion pathways at planes where such faults occur.
(5) The presence or absence of detrital material left in the channels, or introduced subsequently by chemical means such as silanation [17].
(6) The presence or absence of other strongly held guest molecules such as salts [18], water or ammonia [19] introduced intentionally in metered amounts.

Situations have been abundantly demonstrated in which one molecular species is totally excluded, while another is readily sorbed by the same zeolite [20]. This situation often leads to quantitative sieving of one species from the other in a single step, and has proved to be of great significance in large-scale separations and in shape-selective catalysis [21]. In Table V, sieve characteristics have been summarised for three zeolites having 8-ring, 10-ring and

Table V. Sieve characteristrics of a narrow-, an intermediate- and a wide-port zeolite

	Zeolite		
	Ca-A	ZSM-5	Faujasite (zeolites X and Y)
Access of guest through:	8-rings	10-rings	12-rings
Free dimensions[a] of rings (Å)	4.1	5.6 × 5.4 (straight channels) 5.5 × 5.1 (sinusoidal channels)	7.4
Channel system	3-dimensional	3-dimensional	3-dimensional
Sorbed	*n*-paraffins	*n*- and simple *iso*-paraffins benzene, toluene, xylenes, 1,2,4-trimethylbenzene, naphthalene	*n*-, *iso*-, *neo*- and *cyclo*-paraffins, many aromatics including 1,3,5-triisopropyl-benzene
Dimension critical for entry (Å)	~4.9	up to ~6.9	up to ~8.8
Excluded	*Iso*-, *neo*- and *cyclo*-paraffins and aromatics	Pentamethyl- and 1,3,5-tri-methylbenzene	*n*-perfluorotripropylamine
Critical dimension of excluded guest (Å)	~5.6	~7.8	~10

[a] Assuming 2.75 Å as the diameter of framework oxygens.

Table VI. Diffusivities D in cm^2s^{-1} for gases in K-mordenite at −78 °C [22]

Species	Dimensions (Å)	D	$D = D_o \exp - E/RT$	
			$D_o(cm^2s^{-1})$	E(kcal mol^{-1})
H_2	2.4×3.1	2.7×10^{-13}	$1.6_4 \times 10^{-10}$	2.5
O_2	2.8×3.9	2.0×10^{-15}	$1.5_9 \times 10^{-10}$	4.4
N_2	3.0×4.1	9.2×10^{-16}	2.0×10^{-10}	4.8
Ar	3.8_3	2.4×10^{-16}	5.6×10^{-7}	8.4
Kr	3.9_4	1.8×10^{-18}	$2.5_6 \times 10^{-7}$	10.0

12-ring windows controlling sorption. These represent so-called narrow port, intermediate port and wide port zeolites. 8-, 10- and 12-ring windows can be variously distorted to crown, boat or chair shapes, with differing free dimensions which diversify further the types of sieve available. Further, the free dimensions can be changed by the other factors listed above. For example, when Ca−A is converted to Na−A the 8-ring windows are partially obstructed by the Na^+ ions and the zeolite will no longer sorb *n*-paraffins from propane upwards at or near room temperature. It can still sorb small molecules like O_2 or N_2.

Diffusion coefficients can be remarkably sensitive to the molecular dimensions of the guest molecules, even where the differences in dimensions are quite small. This is illustrated in Table VI for simple gases diffusing in K-mordenite at −78 °C [22]. In going from H_2 to Kr there is a 10^5-fold decrease in diffusivity, D, and a four-fold increase in the energy barrier involved in each unit diffusion process. Molecules having dimensions somewhat larger than the free dimensions of the windows, can penetrate the crystals, especially at higher temperatures, because neither the guest molecules nor the oxygen atoms lining the inner peripheries of the windows are like hard spheres, and because of breathing frequencies among the vibrations involving the windows.

4. Zeolite and Clathrate Host Structures – a Comparison

Distinctions between zeolite and clathrate host lattices are less marked than their similarities. Thus, to form the porous host structure, in the first instance it must be crystallised in the presence of a guest molecule which occupies the pore space and stabilises the open structure. With zeolites the space filler and stabiliser has always been water; in clathration other guest molecules have served the same purpose.

A difference arises in the strength of the bonds between the lattice-forming units of the host structure. In the zeolites these are so strong that the porous crystals remain rigid and open when the water is removed. They can then sorb appropriate guest species, and can be heated to rather high temperatures without lattice collapse. In clathrates the bonds between lattice-forming units of the host are much weaker. On lowering the pressure and so the equilibrium content of guest there comes a stage where the whole complex dissociates and the porous β-phase of the host collapses into the compact α-phase. Conversely, on raising the pressure the clathrate will not form until a critical pressure is reached. At this pressure the equilibrium content of guest species is sufficient to stabilise the β-phase and clathration can take place. Thus, for clathration one obtains only part of the sorption isotherm, as illustrated for Kr in phenol in Figure 6, whereas in a zeolite the complete isotherm is measured, as shown for CF_4 in faujasite in Figure 7. In both cases, however, the isotherms, or those parts which are realisable, are of the same form, which is Type I in Brunauer's classification.

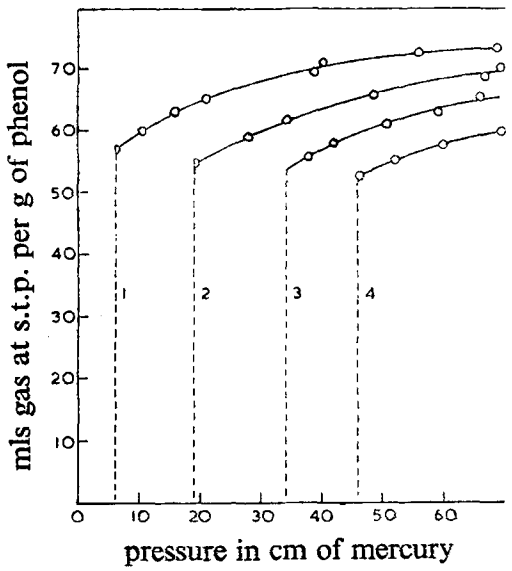

Fig. 6. Isotherms for sorption of Kr in phenol [22a]. Curve 1, 195 K; curve 2, 212 K; curve 3, 222.2 K; curve 4, 228 K.

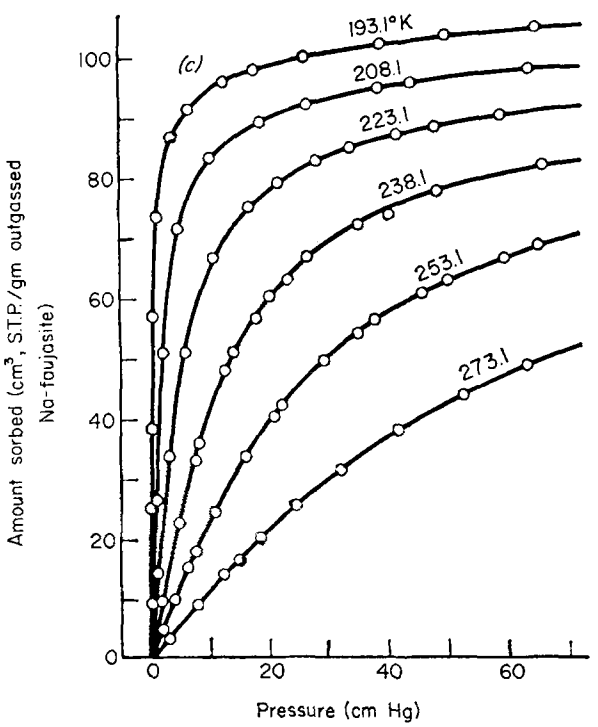

Fig. 7. Isotherms for sorption of CF_4 in zeolite Na–X [22b].

However, even the distinction illustrated in Figures 6 and 7 is not always found. An open host lattice of $M^{II}[4\text{-methylpyridine}]_4(NCS)_2$ where M^{II} is Co or Ni can readily be formed by clathration with benzene and then removal of this guest by evacuation. The permanently open structure can then sorb freely many gases and vapours [23]. Likewise, when water is removed from $K_2Zn_3[Fe(CN)_6]_2 \cdot xH_2O$ the lattice remains open and copiously sorbs gases and hydrocarbons [24]. It is also found that Dianin's compound (4-p-hydroxyphenyl-2,2,4-trimethyl chroman) crystallises with large hourglass-shaped cavities, whether a guest molecule is present or not, which makes it unique. Especially if it is shaken with small steel ball-bearings, this compound sorbs large amounts of appropriate gases and vapours [25].

5. Types of Zeolite Inclusion Complex

Guest species sorbed by zeolites are remarkably varied in their nature. They may be isolated metal atoms or clusters of atoms; they may be salts; or they may be nonpolar or polar molecular species of every description, subject of course to the shape and size requirement imposed by the mesh of the given zeolite sieve.

5.1. METALS

Metal atoms may be introduced as vapours (Hg and Na); as volatile compounds which after sorption are decomposed by heating (e.g., as metal carbonyls); or by ion exchange followed by reduction, e.g.,

$$Ni^{II}\text{-zeolite} + H_2 \rightarrow H\text{-zeolite} + Ni.$$

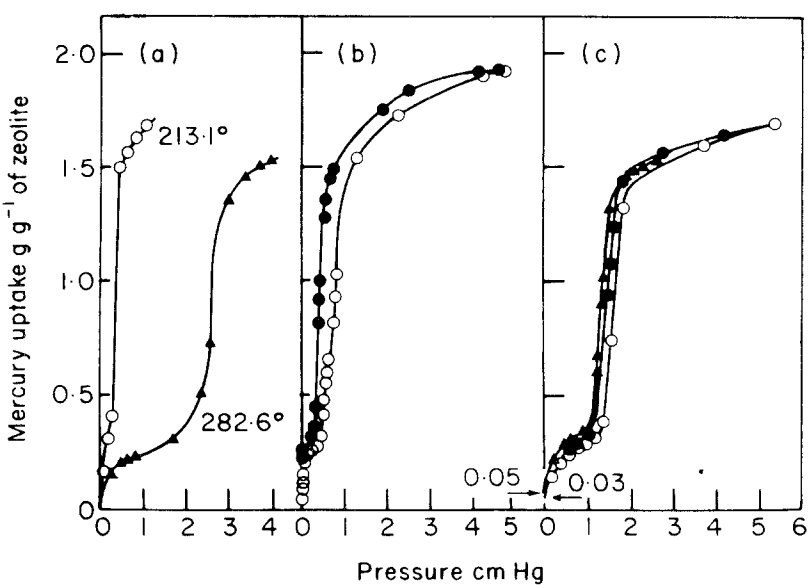

Fig. 8. Sorption of mercury in Ag–X [28]. Temperatures are in °C. ○, ▲ denote sorption points and ● denotes desorption. (a) Sorption branches at two temperatures. (b) Sorption-desorption cycle at 235.2 °C. (c) Two successive sorption-desorption cycles at 270 °C.

When a zeolite containing atomically dispersed metal atoms is heated sufficiently strongly the metal atoms migrate and always show a tendency to form small clusters within the channels and/or crystallites external to the zeolite. Because metal-bearing zeolites are important catalysts, e.g., in Fischer–Tropsch hydrocarbon synthesis, their behaviour has received much attention, especially when Ag, Ni, Co, Pt and Pd are present [26, 27]. The sorption of Hg vapour has been measured quantitatively [28]. When the exchange ion was higher in the electrochemical series than Hg (e.g., Na, Ca, Pb) the mercury was weakly sorbed, like an inert gas. However, when the ion was as low or lower in the series than mercury, the ion was reduced, e.g.,

$$2Ag^{+} + Hg \rightarrow 2Ag + Hg^{2+}$$

$$Hg^{2+} + Hg \rightarrow Hg_2^{2+}$$

and the silver or Hg_2^{2+} appeared to nucleate cluster formation in sorbed mercury which saturated the crystals. The isotherm contours for Hg in Ag–X are illustrated in Figure 8 [28]. The silver zeolites can act as mercury scavengers.

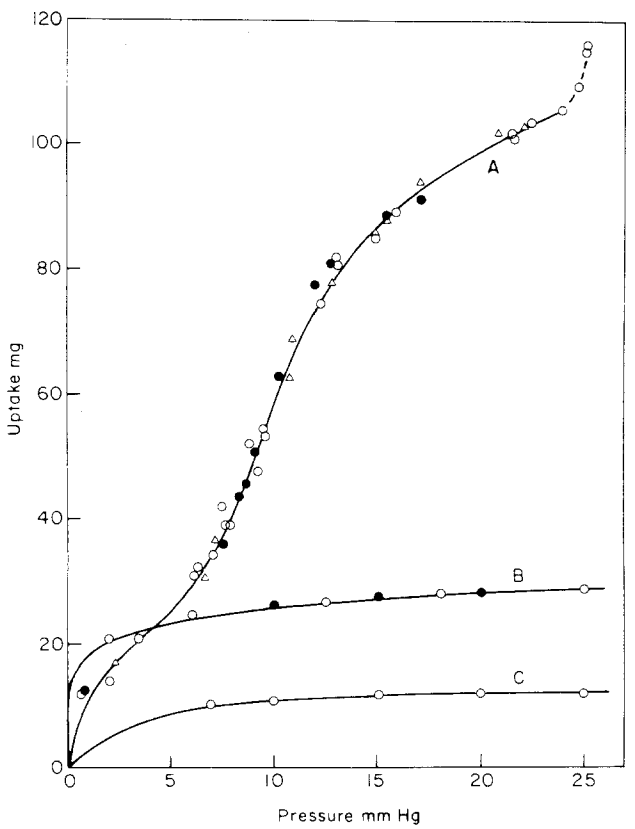

Fig. 9. (A) sorption of NH_4Cl vapour (= NH_3 + HCl) in H-mordenite [32]. (B) NH_3 alone in H-mordenite. (C) HCl alone in H-mordenite. In all cases temperature is 230 °C; ○ denote sorption and ● desorption; △ denote points for final pressures and uptakes.

5.2. SALTS

If outgassed zeolite crystals are stirred in salt melts or exposed to vapours of volatile salts they take up large amounts of salt, subject to size limits of the ions of the salts. In zeolites with large cavities, such as faujasite (zeolites X and Y) and zeolite A, clusters of salt molecules may be present. Structural studies for several zeolites indicate specific sites for anions and cations within the channels [29, 30, 31]. The isotherms for uptake of vapourised NH_4Cl has the same form as those obtained for Hg in Hg– or Ag–X (Figure 9 [32]). The vapour is NH_3 + HCl in equal amounts, which are co-sorbed with strong molecule–molecule interaction within the zeolite, so that the mixture is much more copiously sorbed than either NH_3 or HCl alone.

5.3. POLAR AND NONPOLAR MOLECULES

Many studies have been made of equilibria, energetics and kinetics of sorption of polar and nonpolar molecules within zeolites, and attention has been given to interpreting the results in terms of molecular events and models. Isotherms normally have the contours indicated in Figure 7. However, as interaction between pairs of guest molecules increases, the isotherms can show an upward inflexion (Xe in Li–X [33]), and in an extreme case can give a very steeply rising part, as seen for phosphorus in Na–X (Figure 10).

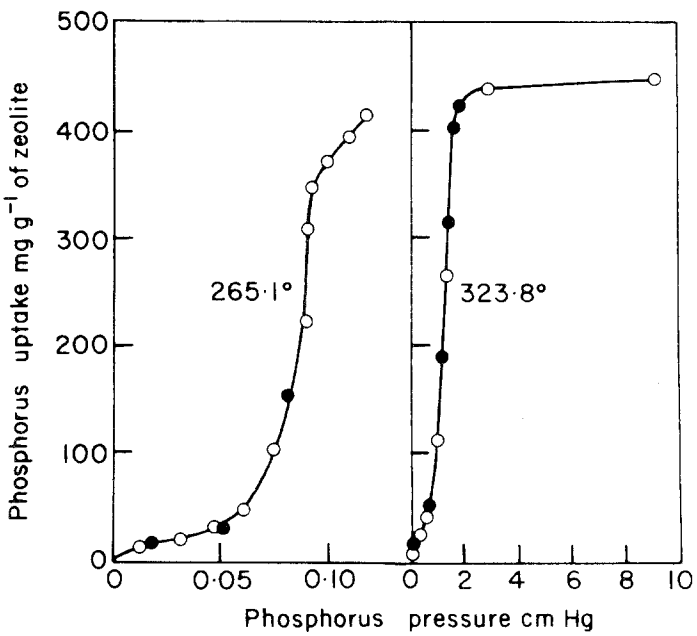

Fig. 10. Isotherms for uptake of phosphorus in Na – X [34].

6. Equilibrium and its Formulation

The distribution equilibrium constant, K, between guest molecules in the gas phase and in the crystals is given in terms of equilibrium activities of guest, a_g in the gas phase and a_s in the crystals, by

$$K = a_s/a_g. \tag{1}$$

With corresponding chemical potentials related to the activities by

$$\mu_s = \mu_s^\theta + RT \ln a_s \qquad \mu_g = \mu_g^\theta + RT \ln a_g \tag{2}$$

one finds from the equilibrium requirement $\mu_s = \mu_g$ that

$$\Delta\mu_s^\theta = \mu_s^\theta - \mu_g^\theta = -RT \ln K \tag{3}$$

where μ^θ is a standard chemical potential. The activity in the gas phase can be measured as a pressure or relative pressure and for a perfect gas gives

$$K_p = a_s/p = c_s \gamma_s/p \tag{4}$$

$$\frac{d \ln K_p}{dT} = \frac{\Delta H^\theta}{RT^2} \tag{5}$$

where c_s and γ_s are the concentration and activity coefficient of guest molecules in the zeolite and ΔH^θ is the standard heat of sorption. In the Henry's law limit ($c_s = K_p p$) $\gamma_s = 1$ and so K_p can be found. Figure 11 shows some plots of $\ln K_p$ *vs* $1/T$ for some gases in H-chabazite [35]. The slopes of these lines give $-\Delta H^\theta/R$, from Equation (5). Also outside the Henry law region one has from Equation (4)

$$\gamma_s = K_p(p/c_s) \tag{6}$$

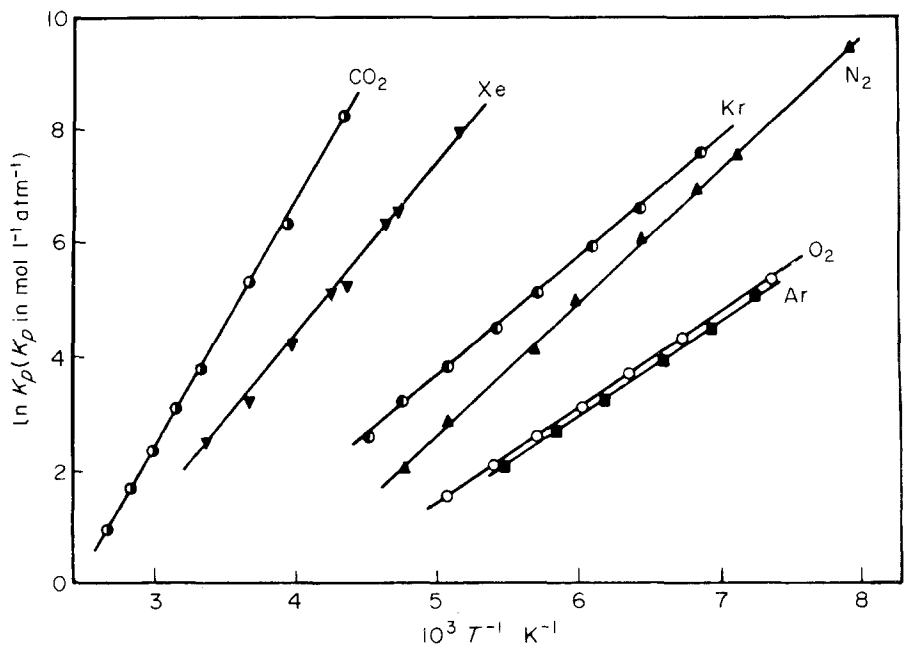

Fig. 11. Plots of $\ln K_p$ against reciprocal absolute temperature for some gases in H-chabazite [35].

Figure 12 [35] shows how γ_s depends on c_s (mol dm^{-3}) again for some gases in H-chabazite. The behaviour of γ_s is a sensitive test of isotherm models, each of which predicts a particular dependence of γ_s or a_s upon c_s or upon $\theta = c/c_{sat}$ where c_{sat} is the saturation uptake of guest by host. Thus, Table VII gives expressions for γ_s for a series of model isotherms, for the first

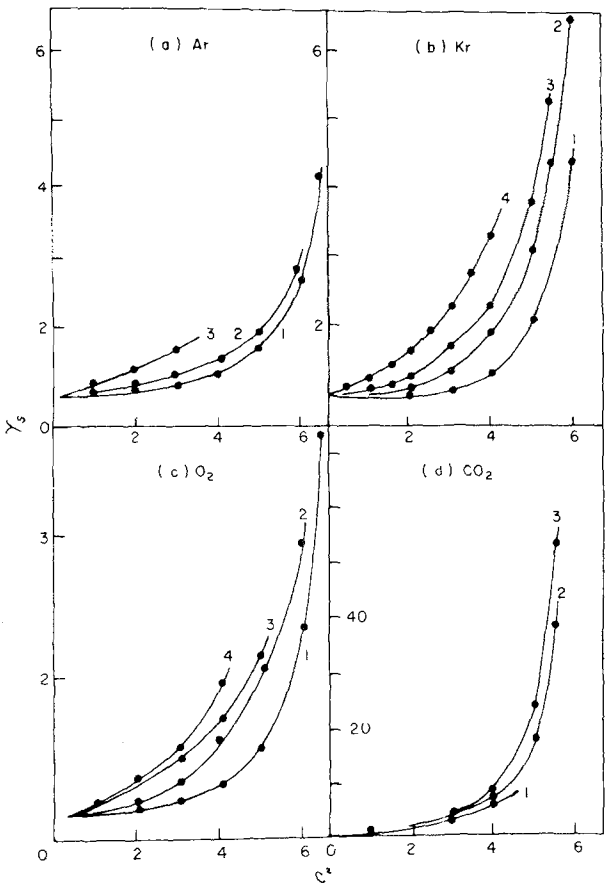

Fig. 12. Activity coefficients for gases in H-chabazite as functions of C_s (mol dm^{-3}) [35]. (a): (1) 137.8K; (2) 151.7K; (3) 183.2K; (b): (1) 144.9K; (2) 163.1K; (3) 183.8K; (4) 209.2K (c): (1) 135.2K; (2) 156.4K; (3) 165.4K; (4) 175.2K (d): (1) 229.6K; (2) 252.6K; (3) 298.2K.

Table VII. Activity coefficients according to several model isotherms

Model	$\gamma_s = K_p(p/c_s) = K(p/\theta)$	Model No.
Ideal localised sorption (Langmuir)	$1/(1-\theta)$	(1)
Localised sorption with pairwise interaction (Lacher; Fowler and Guggenheim)	$1/(1-\theta)\left\{\frac{2-2\theta}{\beta+1-2\theta}\right\}^z$	(2)
Quasi-chemical approximation to localised sorption with pairwise interaction	$[1/(1-\theta)]\exp\left[\frac{2w\theta}{RT}\right]$	(3)
Volmer equation of state for sorbed fluid $(P(V-b)=RT)$	$[1/(1-\theta)\exp[\theta/(1-\theta)]$	(4)
Van der Waals equation of state for sorbed fluid $(P+a/V^2)(V-b)=RT$	$[1/(1-\theta)]\exp[\theta/(1-\theta)-\alpha\theta]$	(5)
Virial equation of state for sorbed fluid $(P/(c_sRT)=1+A_1c_s+A_2c_s^2+A_3c_s^3+\ldots)$	$\exp\{2A_1c_s+(3/2)A_2c_s^2+(4/3)A_3c_s^3+\ldots\}$	(6)

five of which the equilibrium constants K_p (Equation (4)) and K (Equation (1)) are related by

$$K_p = Kc_{sat} \tag{7}$$

For model 6 with $a_g = p$ (perfect gas) $K_p = K$ and for all six models γ_s is obtained from Equation (6).

For localised sorption with interaction (models 2 and 3) z is the coordination number of each identical sorption site; $2w/z$ is the interaction energy between a pair of adjacent molecules*; and β is given by

$$\beta = [1 - 4\theta(1 - \theta)\{1 - \exp(-2w/zRT)\}]^{1/2} \tag{8}$$

For models 4, 5 and 6 the guest molecules are regarded as filling the intrazeolitic volume at a mean hydrostatic stress intensity P when the concentration is c_s; V is the molar volume of the guest at concentration c_s; a and b have a similar significance, but not necessarily identical values, to these coefficients for the guest species in bulk; and $\alpha = 2a/bkT$. In model 6, the A_i (i = 1,2,3...) are coefficients which may depend on temperature but are independent of c_s.

Table VIII. Comparison of experimental γ_s and γ_s calculated from model isotherms for C_2H_6 at O °C in H-chabazite [36] [a]

$10^{-3}c_s$ / mol m^{-3} of crystal	Exptl	Model 1	Model 3 ($2w/RT = -0.5$)	Model 4	Model 5 ($\alpha = 1$)	Model 6 [b]
0.5	1.16	1.15	1.08	1.34	1.18	1.18
1.0	1.38	1.36	1.19	1.97	1.50	1.38
1.5	1.70	1.67	1.36	3.27	2.19	1.68
2.0	2.22	2.15	1.4	6.8	3.9_9	2.23
2.5	3.16	3.03	2.17	22.9	11.7	3.4_1
3.0	6.35	5.9_8	3.0	30.1	13.5	6.3
3.5	22.9	15.8_7	9.9_4	4.5×10^7	1.8×10^7	14.8

[a] The H-chabazite was ~75% crystalline [35]. c_{sat} for pure H-chabazite was taken as 3.74×10^3 mol m^{-3}

[b] $A_1 = 1.87 \times 10^{-4}$ (mol m^{-3})$^{-1}$; $A_2 = -8.0 \times 10^{-8}$ (mol m^{-3})$^{-2}$; $A_3 = 50.0 \times 10^{-12}$ (mol m^{-3})$^{-3}$.

Table VIII compares the experimental values of γ_s for C_2H_6 sorbed at 0 °C in H-chabazite with values calculated from models 1 to 6 using selected values of the adjustable parameters. The best fits were obtained with Langmuir's model for ideal localised sorption (model 1), and the virial isotherm equation [37] (model 6). Models 4 and 5, based upon the oversimple Volmer and van der Waals equations of state, lead to unsatisfactory representations of experimental behaviour.

The Langmuir isotherm equation and that of model 3 may be tested in another sensitive way by plotting $\theta/[p(1 - \theta)]$ or its logarithm against θ or c_s. If the Langmuir isotherm is valid the plot will be a straight line parallel with the axis of c_s. Examples of such semi-log plots often show negative, nearly zero, or positive slopes at low, intermediate and high temperatures respectively, at least over part of the range $0 < \theta \leq 1$. Positive slopes could correspond with negative values of $2w\theta/RT$ in model 3, which should decrease as T rises. However, negative slopes would not appear unless w changed from negative to positive as T decreased. Other factors, such as the well-established energetic heterogeneity of many zeolite sorbents, must

* Interactions of all save nearest neighbour pairs are ignored.

play a part. One may conclude that the localised models of Table VII do not give more than a qualitative or semi-quantitative description of sorption equilibrium in zeolites, and that only the virial isotherm, among those based on equations of state, is likely to be of use for concentrated zeolite solutions.

A further attempt was made to remove some of the artificiality of the site concepts of Langmuir by considering each cavity in zeolites such as A or X as a single sorption site which is capable of binding a maximum of m molecules (cf. Table IV). Detailed balancing [38] or statistical mechanics [39] both lead to an isotherm of the form

$$\theta = \frac{r_1 \left\{ 1 + (m-1)r_2 + \dfrac{(m-1)(m-2)}{(1.2)} r_2 r_3 + \cdots + (r_2 r_3 \cdots r_m) \right\}}{1 + m r_1 + \dfrac{m(m-1)}{(1.2)} r_1 r_2 + \cdots + (r_1 r_2 \cdots r_m)} \tag{9}$$

where $r_i = (k_{(i-1)}/k_i)p$. $k_{(i-1)}$ is the rate constant for condensation of a molecule into a cavity holding a cluster of $(i-1)$ molecules and k_i is the rate constant for desorption from the cavity holding a cluster of i molecules. The k's may, in principle, be functions of cluster size; for example, if there are molecule–molecule interactions between pairs of the guest molecules. If the k's are independent of cluster size (and so of θ), the isotherm reduces to that of Langmuir for ideal localised sorption. An interest in this treatment is that one does not require one guest molecule per site, and that the site (here the cavity) accommodates molecules in different numbers according to their size. If the maximum number of guest molecules per cavity for a given molecule is $m = 2$, no terms beyond that in r_2 need to be included in the isotherm equation. If $m = 1$, the Langmuir isotherm is again recovered. It is of interest that for C_{10} to C_{18} n-paraffins not more than one of these molecules can be accommodated per cavity in zeolite A, and that the isotherms are reasonably well represented by Langmuir's isotherm [40]. It may be that each n-paraffin tends to coil up in its cavity to give a rather globular form, and that then there is no room per cavity for more than one of these coiled molecules, irrespective of carbon number. The sorbent with one guest molecule per cavity could be also much more energetically uniform and so conform better with Langmuir's postulates. One molecule per cavity corresponds with a simple interstitial solid solution. In treating clathration, exemplified by the uptake of simple gases in β-quinol, van der Waals and Platteeuw [41] also arrived at Langmuir's isotherm equation. The equilibrium clathrate solutions they considered also had one guest molecule per cavity.

7. Concluding Remarks

One may summarise certain of the complexities which one would need to consider in a full treatment of intrazeolitic sorption equilibrium as follows:

(i) Apparent saturation uptakes decrease for a given guest species as the temperature, T, increases. Thus co-volumes of guest molecules tend to increase with T just as they do in bulk liquid or solid.

(ii) Coefficients of thermal expansion of guest molecules, present as clusters or as filaments in the intrazeolitic channel systems, are not very different from those of the corresponding bulk liquids.

(iii) Fewer large molecules than small ones saturate the pore space in the crystals. Thus classical models of equilibrium involving one molecule per site are inadequate in that the

so-called site, and the number of sites, would need to be different according to the molecular volume of each guest.

(iv) In molecular clusters or filaments the guest molecules are not all bound with the same energy. This binding energy varies with the position of the guest relative to the walls of the cavities and to the exchange cations within the zeolite.

(v) Molecule–molecule interaction within the zeolite may and often does modify the equilibrium uptakes and the differential heats of sorption for a given uptake.

In the light of the above properties the approaches made (cf. Table VII and Equation (9)) are unlikely to achieve more than partial success. The first two of these properties suggest that the best treatment will consider the guest within the zeolite as fluid-like. However, the last two mean that the treatment has to deal with a non-homogeneous fluid, especially at low uptakes. The treatments leading to the isotherm equation of the form shown in Equation (9) avoid the problem (iii) for the site model, and the statistical mechanical formulation allows in principle for (iv) and (v) to be included. However, the evaluation of the way in which energy varies with position and of the self-potential is very difficult to achieve. The theory of the physical bond is, for *a priori* calculations, not very different from that of the chemical bond is its state of advancement. Both are at best semiquantitative. It is therefore encouraging and even surprising to find the degree of success in understanding equilibrium which has been achieved.

References

1. R. M. Barrer: *Zeolites and Clay Minerals as Sorbents and Molecular Sieves*, Chap. 2. Academic Press, (1978).
2. D. E. Appleman: Amer. Cryst. Assoc., Mineral. Soc. America, Joint Meeting, Gatlinburg, Tenn., 1965, p. 80.
3. E. M. Flanigen, J. M. Bennett, R.W. Grose, J. P. Cohen, R. L. Patton, R. M. Kirchner, and J. V. Smith: *Nature* **271**, 512 (1978).
4. D. M. Bibby, N. B. Milestone, and L. P. Aldridge: *Nature* **280**, 664 (1979).
5. H. K. Beyer and I. Belanykaja: in *Catalysis by Zeolites* (Eds. B. Imelik *et al.*), p. 203, Elsevier (1980).
6. J. L. Schlenker, F. G. Dwyer, E. E. Jenkins, W. J. Rohrbaugh, G. T. Kokotailo and W. M. Meier: *Nature* **294**, 340 (1981).
7. Mobil Oil Corp.: Neth. Patent 7,014,807 (1972).
8. R. J. Argauer and G. R. Landolt: U.S. Patent 3,702,886 (1972).
9. W. M. Meier and D. H. Olson: *Atlas of Zeolite Structure Types*, p. 67, Structure Commission of Int. Zeolite Assoc. (1978).
10. Ref. [9], p. 63.
11. Ref. [9], p. 37.
12. Ref. [1], p. 37.
13. Ref. [1], p. 36.
14. Ref. [1], p. 38.
15. R. M. Barrer and D. E. Vaughan: *J. Phys. Chem. Solids* **32**, 731 (1971).
16. R. M. Barrer: in *Non-stoichiometric Compounds*, (Ed. L. Mandelcorn), p. 393, Academic Press (1963).
17. R. M. Barrer and A. Sikand: *J. Chem. Soc. Faraday* I **75**, 2221 (1979).
18. R. M. Barrer, D. A. Harding, and A. Sikand: *J. Chem. Soc. Faraday* I **76**, 180 (1980).
19. R. M. Barrer and L. V. C. Rees: *Trans. Faraday Soc.* **50**, 852 (1954).
20. Ref. [1], Chap. 1.
21. P. B. Weisz: *Pure Appl. Chem.* **52**, 2091 (1980).
22. R. M. Barrer: *Trans. Faraday Soc.* **45**, 358 (1949);

22a. S. Allison and R. M. Barrer, *Trans. Faraday Soc.* **64**, 549 (1968);

22b. R. M. Barrer and P. J. Reucroft: *Proc. Roy. Soc.* **258A**, 431 (1960).

23. S. A. Allison and R. M. Barrer: *J. Chem. Soc. A* 1717 (1969).
24. P. Cartraud, A. Conitot, and A. Renaud: *J. Chem. Soc., Faraday* I **77**, 1561 (1981).
25. R. M. Barrer and V. H. Shansen, *Chem. Commun.* 333 (1976).

26. L. R. Gellens, W. J. Mortier, and J. B. Utterhoeven: *Zeolites* **1**, 11, 85 (1981).
27. P. Gallezot in *Catalysis by Zeolites* (Eds. Imelik *et al.*), p. 227, Elsevier (1980).
28. R. M. Barrer and J. L. Whiteman: *J. Chem. Soc., A* 19 (1967).
29. R. M. Barrer and H. Villiger: *Z. Kristallogr.* **142**, 82 (1975).
30. R. M. Barrer and D. J. Robinson: *Z. Kristallogr.* **135**, 374 (1972).
31. N. Petranovic, U. Mioc, M. Susic, R. Dimitrijevic, and I. Krstanovic: *J. Chem. Soc. Faraday* I **77**, 379 (1981).
32. R. M. Barrer and A. G. Kanellopoulos: J. Chem. Soc., A 775 (1970).
33. R. M. Barrer and J. L. Whiteman: *J. Chem. Soc., A* 13 (1967).
34. A. V. Kiselev: *Molecular Sieve Zeolites* II (Adv. in Chem. Series 102), p. 43, Amer. Chem. Soc. (1971).
35. R. M. Barrer and J. A. Davies: *Proc. Roy. Soc.* **320A**, 289 (1970).
36. R. M. Barrer and J. A. Davies: *Proc. Roy. Soc.* **322A**, 1 (1971).
37. Ref. [1], p. 131.
38. Ref. [1], p. 145.
39. P. Brauer, A. A. Lopatkin, and G. Ph. Stepanez in *Molecular Sieve Zeolites II* (Adv. in Chem. Series 102) Amer. Chem. Soc., p. 97 (1971).
40. K. Fiedler, A. Roethe, K.-P. Roethe, and D. Gelbin: *Z. Phys. Chem. (Leipzig)* **259**,979 (1978).
41. J. H. van der Waals and J. C. Platteeuw: *Adv. Chem. Phys.* **2**, 1 (1959).